

Effects of the off-center position of the Li^+ ion on the optical properties of the F_A center in KCl

G. Baldacchini and G. P. Gallerano

*Dipartimento Tecnologie Intersectoriali di Base, Divisione Fisica Applicata,
Comitato Nazionale per la Ricerca e per lo Sviluppo dell'Energia Nucleare e delle Energie Alternative,
Centro Ricerche Energia Frascati, Casella Postale 65, 00044 Frascati, Italy*

U. M. Grassano

Dipartimento di Fisica, Seconda Università di Roma, 00173 Roma, Italy

A. Lanciano, A. Scacco, and F. Somma*

Dipartimento di Fisica, Università "La Sapienza," 00185 Roma, Italy

M. Meucci[†] and M. Tonelli

Dipartimento di Fisica, Università di Pisa, 56100 Pisa, Italy

(Received 12 August 1985)

The off-axis symmetry of the F_A center in $\text{KCl}:\text{Li}^+$ has been investigated by optical experiments. We have studied static and dynamic reorientational properties of the F_A center by measurements of absorption and emission. The off-axis model of the center has been confirmed. A theoretical treatment, which takes into account the small deviation of the center with respect to the crystal axes, is in good agreement with the experimental results. Best fittings of the theory to the experimental data yield a value of the off-axis angle $\theta = 8^\circ$.

I. INTRODUCTION

Color centers in alkali halides have been deeply studied in the past as prototypes of point defects in solids. In particular, the F and F_A centers, which are the simplest defects, have been the object of detailed investigations that have also led to the understanding of more complex centers.^{1,2} In the last ten years the interest on these centers has been further stimulated by the possibility of using these defects as active centers in tunable laser systems.³ These lasers possess very useful features, such as high single-mode output, narrow linewidth and a broad tuning range, and their wide field of application, from laser chemistry to high-resolution spectroscopy, from pollution detection to optical communications, explains the increasing number of studies in this research area.

Various types of point defects in doped alkali halides have been successfully tested for laser action, yielding tunability over the spectral range from 0.8 to 4 μm . These defects are formed by F centers associated to impurities, such as Li^+ , Na^+ , and Tl^+ or by ionized pairs of F centers, such as F_2^+ possibly stabilized by neighboring impurities.³⁻⁵ Despite the long list of laser-active centers, the $F_A(\text{II})$ center in $\text{KCl}:\text{Li}^+$, which was the first system showing laser action,^{6,7} is still one of the most widely used, because of its peculiar characteristics of easy production, stability, and low bleaching effects.

The $F_A(\text{II})$ center is formed by an F center (an electron trapped by an anion vacancy) in which one of the six alkali-metal nearest-neighbor ions is replaced by some lighter alkali-metal ion. The optical behavior of the $F_A(\text{II})$ center has been extensively studied, and the

theoretical model currently accepted accounts very well for its optical absorption and emission properties.⁸ The peculiar optical cycle of the $F_A(\text{II})$ center stems from the so-called ionic saddle-point configuration of the defect in the relaxed excited state, in which the electron is shared between two symmetrical potential wells. This configuration, which gives rise to an emission having a large Stokes shift, narrow bandwidth, and short lifetime, is caused by the small size of the substitutional Li^+ ion neighboring the vacancy. However, the precise location of the Li^+ ion in the KCl lattice has not yet been well established, even in the ground-state configuration. Indeed, several small monovalent impurity ions, such as Cu^+ , Ag^+ , and Li^+ , introduced substitutionally in alkali halides with sufficiently large lattice parameters, can occupy an off-center position.⁹ The origin of this effect was identified by Matthew¹⁰ as the small size of the substitutional ion, which has a weak overlap interaction with its neighbors. For this reason the repulsive interactions are not strong enough to oppose the displacement of the impurity ion to an off-center position, which is stabilized by the energy gain due to the polarization of the lattice. It is known, for example, that an isolated substitutional Li^+ impurity in KCl occupies an off-center position shifted from the proper lattice site along one of the eight equivalent $\langle 111 \rangle$ directions.¹¹

A similar off-center behavior was suggested to explain Raman experiments in the $F_A(\text{Li})$ centers in KCl.¹² Clear evidence of the off-center displacement of the Li^+ ion in the F_A center was obtained by Rosenberger and Lüty^{13,14} with a detailed analysis of electro-optical experiments. They conclude that the Li^+ ions are displaced into four

equivalent sites, along the $\langle 110 \rangle$ directions, on a plane perpendicular to the symmetry axis of the center. This model has been successfully applied to the interpretation of the results of spin relaxation, yielding information on the tunneling structure of the Li^+ ion.¹⁵ However, contrary to the behavior of isolated off-center impurities, the Li^+ ion of the F_A center in KCl could not be constrained in the on-center position by applying hydrostatic pressure.¹⁶

Because of the fast tunneling motion among the four equivalent positions, it seemed that optical and electron-nuclear double-resonance (ENDOR) experiments could not differentiate between a C_{4v} symmetry and an off-axis geometry.² In particular, the absorption and luminescence properties were expected to be independent of the off-axis displacement of the Li^+ ions. However, careful measurements of luminescence in colored $\text{KCl}:\text{Li}^+$ crystals performed under certain optical pumping configurations have shown unexpected results.¹⁷ Therefore we have started a series of systematic experiments in order to clarify the role of the off-axis configuration. We have found that the absorption, emission, and kinetics of the center reorientation are all affected by the displacement of the Li^+ ion from the lattice site.

In the following section the theoretical model of the optical reorientation of the centers, which takes into account their off-axis angle, is briefly sketched. The experimental apparatus is described in Sec. III, and the discussion of the experimental results reported is in Sec. IV. The conclusions in Sec. V will stress the point that, besides supplying a new technique for studying the properties of the off-axis centers, the orientational behavior of the defects may be used to improve the performances of the $F_A(\text{II})$ color-center lasers.

II. THEORETICAL MODEL

The F_A center model is shown in Fig. 1. In $\text{KCl}:\text{Li}^+$ the F_A center exhibits two absorption bands. The F_{A1} band, peaking at about 630 nm, is due to the dipole transition parallel to the center axis, arrow 1 in Fig. 1, and the twofold degenerate F_{A2} band, peaking at about 550 nm, is due to the dipole transitions perpendicular to the center axis, arrow 2 in Fig. 1. The $F_A(\text{Li})$ emission in KCl consists of one band centered at about $2.7 \mu\text{m}^2$. As is well known, a reorientation process takes place after the optical excitation of the $F_A(\text{II})$ center. This is caused by the possible jumping of the vacancy around the Li^+ ion during the relaxation process. As a consequence, optical pumping within the F_{A1} band with light polarized along one of the three $\langle 100 \rangle$ directions leads to the alignment of the centers along the other two perpendicular directions, where they can no longer be excited [Fig. 2(a)]. On the other hand, if the same pumping beam is polarized at 45° with respect to the crystal x and y directions, then all centers will be aligned preferentially along the z direction [Fig. 2(b)]. Such a reorientation process is temperature independent for $F_A(\text{II})$ centers, with a reorientation quantum efficiency $\eta = 0.5$.²

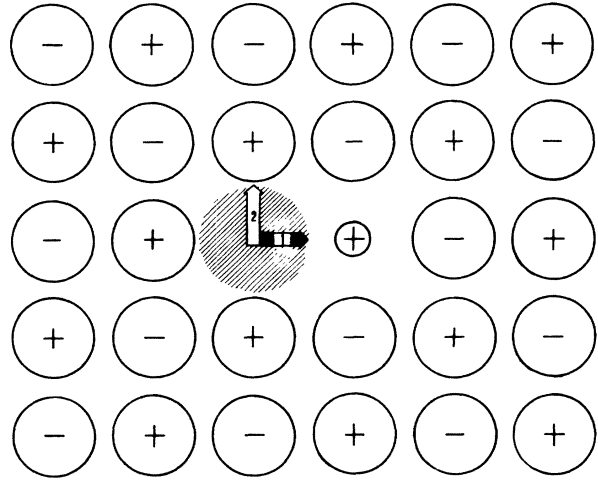


FIG. 1. Ionic configuration of the F_A center in alkali halides with absorption transition vectors.

If the centers are not exactly aligned along the directions of the crystallographic axes, because of the off-center displacement of the Li^+ ions, then both alignment processes described above cannot be fully achieved. Indeed, in this case all the reoriented centers can still be excited, although with a smaller probability, proportional to the square of the component of the electric field of the incident light along the direction of the center dipoles. As a consequence, a dynamical equilibrium is established, in which none of the initial center directions are completely depopulated.

Let us now calculate the time evolution under polarized optical pumping of intensity I_0 of the number of centers, N_i , lying along the four directions forming the angle θ with the crystallographic axis i ($i = x, y, z$). Indicating by σ_i the relative absorption cross sections of the centers, we have

$$\begin{aligned} \frac{1}{\eta I_0} \frac{dN_x}{dt} &= -\sigma_x N_x + \frac{\sigma_y N_y}{2} + \frac{\sigma_z N_z}{2}, \\ \frac{1}{\eta I_0} \frac{dN_y}{dt} &= \frac{\sigma_x N_x}{2} - \sigma_y N_y + \frac{\sigma_z N_z}{2}, \\ \frac{1}{\eta I_0} \frac{dN_z}{dt} &= \frac{\sigma_x N_x}{2} + \frac{\sigma_y N_y}{2} - \sigma_z N_z, \end{aligned} \quad (1)$$

where the numerical factor $\frac{1}{2}$ stems from the fact that the centers leaving one direction can reorient themselves on the other two directions with equal probability. Of course, the total number of centers in the crystal is constant, i.e.,

$$N = N_x + N_y + N_z. \quad (2)$$

The absorption cross section of the various centers is proportional to $|\hat{\mathbf{e}} \cdot \mathbf{r}|^2$, where $\hat{\mathbf{e}}$ is a unit vector showing the direction of the polarization of the incident light beam and \mathbf{r} is the transition dipole moment, whose direction for the F_{A1} transition is parallel to the center axis. Assuming that the pumping F_{A1} light propagates along the z axis,

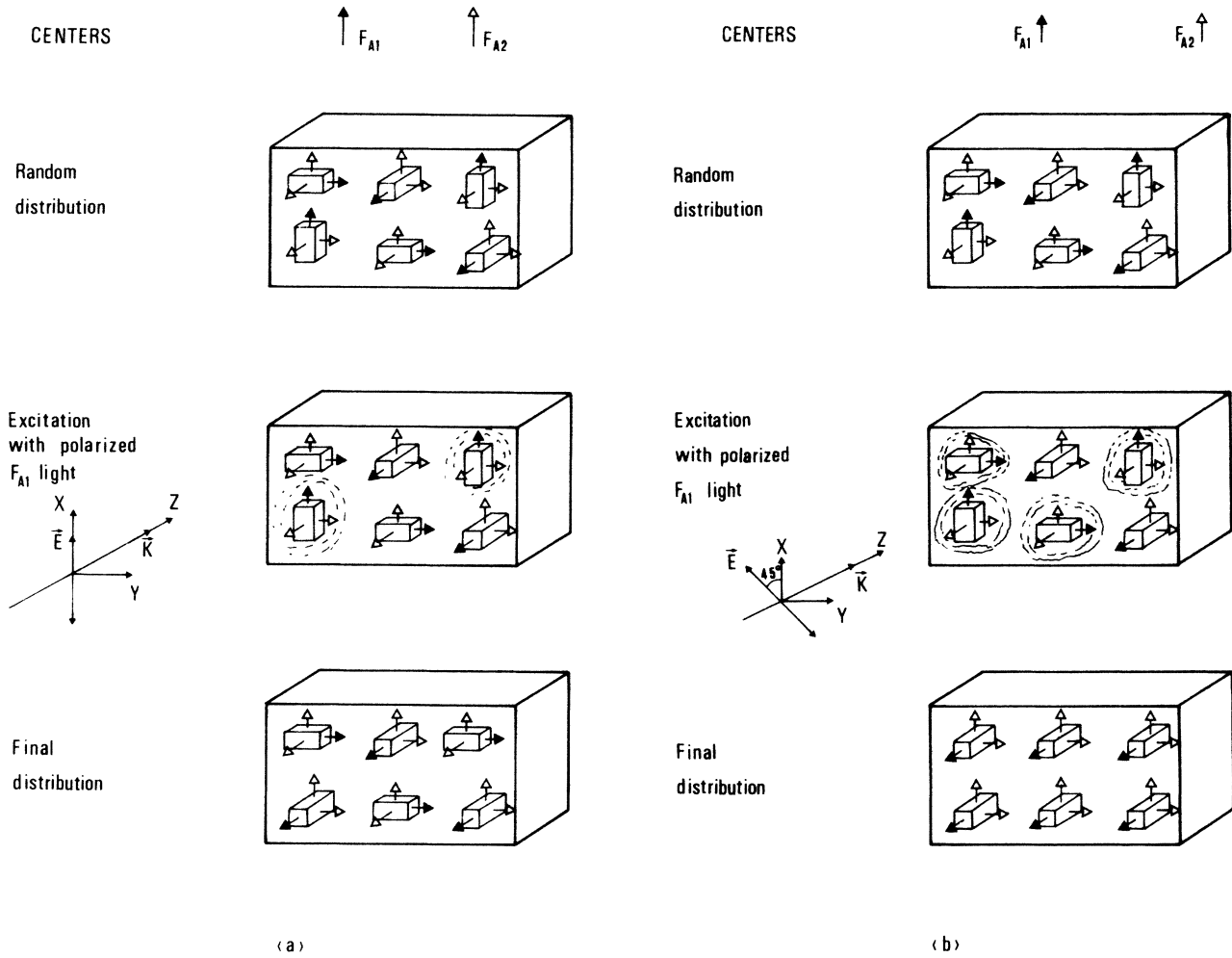


FIG. 2. F -center reorientation under optical excitation: (a) polarization parallel to one of the crystal axes; (b) polarization at 45° with respect to two crystal axes.

and indicating by ξ the angle between \hat{e} and the x axis and by θ the off-axis angle of the $F_A(\text{Li})$ center (see Fig. 3), the absorption cross section σ_i can be obtained by averaging the amount $|\hat{e} \cdot \mathbf{r}|^2$ over the four possible orientations of the centers around the i axis. We obtain

$$\begin{aligned} \sigma_x &= \sigma_0(\cos^2\theta \cos^2\xi + \frac{1}{2} \sin^2\theta \sin^2\xi), \\ \sigma_y &= \sigma_0(\cos^2\theta \sin^2\xi + \frac{1}{2} \sin^2\theta \cos^2\xi), \\ \sigma_z &= \frac{1}{2} \sigma_0 \sin^2\theta, \end{aligned} \quad (3)$$

where σ_0 is the absorption cross section of an on-axis center. Equations (3) have been obtained under the hypothesis of even distribution of centers among the four equivalent positions around the symmetry axis (Fig. 3). This approximation is fully justified, because the tunneling processes among these four equivalent configurations have a typical frequency of the order of 10^8 s^{-1} ,¹⁴ much larger than the optical pumping rate used in our experiments.

The general solutions of Eqs. (1) can be written as

$$\begin{aligned} N_x(t) &= \frac{N\sigma_y\sigma_z}{\sigma_x\sigma_y + \sigma_x\sigma_z + \sigma_y\sigma_z} - C_1 \frac{\sigma_z - \sigma_x + \Delta}{\sigma_y - \sigma_x} \exp\left[-\frac{A - \Delta}{2} \eta I_0 t\right] - C_2 \frac{\sigma_z - \sigma_x - \Delta}{\sigma_y - \sigma_x} \exp\left[-\frac{A + \Delta}{2} \eta I_0 t\right], \\ N_y(t) &= \frac{N\sigma_x\sigma_z}{\sigma_x\sigma_y + \sigma_x\sigma_z + \sigma_y\sigma_z} + C_1 \frac{\sigma_z - \sigma_y + \Delta}{\sigma_y - \sigma_x} \exp\left[-\frac{A - \Delta}{2} \eta I_0 t\right] + C_2 \frac{\sigma_z - \sigma_y - \Delta}{\sigma_y - \sigma_x} \exp\left[-\frac{A + \Delta}{2} \eta I_0 t\right], \\ N_z(t) &= \frac{N\sigma_x\sigma_y}{\sigma_x\sigma_y + \sigma_x\sigma_z + \sigma_y\sigma_z} + C_1 \exp\left[-\frac{A - \Delta}{2} \eta I_0 t\right] + C_2 \exp\left[-\frac{A + \Delta}{2} \eta I_0 t\right], \end{aligned} \quad (4)$$

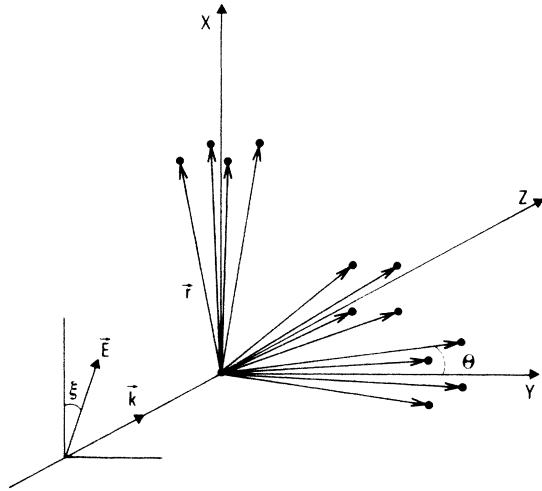


FIG. 3. Model showing the orientations of the transition dipole moments of the F_A centers, \mathbf{r} , with respect to the electric field \mathbf{E} of the incoming em radiation.

where

$$A = \sigma_x + \sigma_y + \sigma_z ,$$

$$\Delta = [\sigma_x(\sigma_x - \sigma_y) + \sigma_y(\sigma_y - \sigma_z) + \sigma_z(\sigma_z - \sigma_x)]^{1/2} ,$$

and C_1 and C_2 are determined by the initial conditions. Equations (4) allow us to evaluate the absorption and emission of the crystal under various pumping schemes and in both dynamic and static regimes. Indeed, the absorption coefficient is given by

$$\alpha = N_x \sigma_x + N_y \sigma_y + N_z \sigma_z , \quad (5)$$

and the emission intensity is obviously proportional to the absorption coefficient and to the intensity of the pumping radiation.

Information about the off-axis angle θ , which appears in the expressions of the cross section in Eqs. (3), can be obtained from measurements of absorption and emission. In particular, we have found that three schemes of measurement are well suited to be performed experimentally.

A. Steady-state effects

In the case of stationary pumping with em radiation having constant intensity and polarization, the steady-state populations along the three axes are given by

$$N_x = \frac{\sigma_y \sigma_z}{\sigma_x \sigma_y + \sigma_x \sigma_z + \sigma_y \sigma_z} N ,$$

$$N_y = \frac{\sigma_x \sigma_z}{\sigma_x \sigma_y + \sigma_x \sigma_z + \sigma_y \sigma_z} N , \quad (6)$$

$$N_z = \frac{\sigma_x \sigma_y}{\sigma_x \sigma_y + \sigma_x \sigma_z + \sigma_y \sigma_z} N ,$$

and the steady-state absorption α_s is easily calculated:

$$\alpha_s = \frac{3N}{1/\sigma_x + 1/\sigma_y + 1/\sigma_z} . \quad (7)$$

It can be shown by using the relations (3) in Eq. (7) that the absorption is a periodic function of ξ , i.e., $\alpha_s(\xi) = \alpha_s(\xi + \pi/2)$, and it is strongly dependent on the value of the angle θ . Therefore from accurate static measurements of absorption or luminescence it is possible to derive such a value.

B. Transient effects

A second method for the measurement of θ derives from the temporary changes of the absorption coefficient following a sudden change of the pumping conditions.

The sample is irradiated with light polarized at $\xi = 0^\circ$. When the angle ξ is switched abruptly from 0° to $\pi/2$, the initial population remains that established by the previous pumping at $\xi = 0^\circ$. The expression for this initial transient absorption $\alpha_t(0)$ is given by

$$\alpha_t(0) = N\sigma_0 \frac{\sin^4 \theta / 2 + 2 \cos^4 \theta + \sin^2 \theta \cos^2 \theta}{1 + 3 \cos^2 \theta} . \quad (8)$$

When the center orientation reaches the final equilibrium, the absorption $\alpha_t(\infty)$ is given by

$$\alpha_t(\infty) = N\sigma_0 \frac{3 \sin^2 \theta \cos^2 \theta}{1 + 3 \cos^2 \theta} . \quad (9)$$

Keeping in mind that θ is quite small, one obtains, from the ratio of the two expressions,

$$\frac{\alpha_t(\infty)}{\alpha_t(0)} \cong \frac{3 \sin^2 \theta}{1 + \cos^2 \theta} . \quad (10)$$

Therefore the measurements of the initial and final values of this transient absorption (or emission) allows a direct measure of the off-axis angle. Let us note that the value $\alpha_t(\infty)$ coincides with the steady-state absorption $\alpha_s(\xi)$ for $\xi = 0^\circ$.

C. Kinetics measurements

As a last case we consider the time variation of the absorption and emission in a crystal prepared as in Figs. 2(a) and 2(b).

The centers are first oriented along the z direction by pumping with a polarized beam at $\xi = \pi/4$, as in Fig. 2(b). Subsequently, the polarization is rotated abruptly at $\xi = \pi/2$ and the increase of the population along the x axis is monitored independently. From Eqs. (4) it is easily calculated with the appropriate initial conditions that the process exhibits an exponential behavior of the type

$$\alpha(t) \cong \frac{N\sigma_0}{2} (1 - e^{-t/T_S}) \quad (11)$$

where

$$T_S = \frac{2}{\eta I_0 (A - \Delta)} = \frac{4}{3\eta I_0 \sigma_0 \sin^2 \theta} \quad (12)$$

is the time constant of this "slow" process. In deriving

Eq. (11) we have neglected in Eqs. (4) and (5) the terms in $\sin\theta$ of order higher than 2 and, likewise, the other exponential terms of Eqs. (4) that have a negligible coefficient. Secondly, the centers are oriented along the y and z axes, by pumping with a polarized beam at $\xi=0^\circ$, as in Fig. 2(a). If the angle of polarization is switched suddenly to $\xi=\pi/2$, the population of the centers along the y axis decreases exponentially and the absorption is given by

$$\alpha(t) \simeq \frac{N\sigma_0}{2} e^{-t/T_F}, \quad (13)$$

where

$$T_F = \frac{2}{\eta I_0 (A + \Delta)} = (\eta I_0 \sigma_0)^{-1} \quad (14)$$

is the time constant of this "fast" process. In conclusion, the ratio of the two time constants gives

$$T_F/T_S = \frac{3}{4} \sin^2\theta, \quad (15)$$

and again the kinetics of absorption or emission gives direct information on the off-axis angle.

Let us point out that in all three previous cases we have supposed the incident radiation to be of constant intensity in space (inside the crystal) and in time. This condition is not always fulfilled in our experiments, so that various corrections will be introduced later in the paper. However, these corrections do not alter the validity of Eqs. (7), (10), and (15).

III. EXPERIMENTAL APPARATUS

The standard experimental setup used for the absorption and emission measurements is shown in Fig. 4. The crystal thickness used in all optical measurements was 1.0 ± 0.1 mm. The samples were home-grown single crys-

tals of $\text{KCl}:\text{Li}^+$ additively colored in potassium vapor. The formation of the F_A centers was obtained by irradiating the sample at -20°C with green light absorbed by the F centers. The crystals containing F_A centers were cooled in a liquid-helium immersion cryostat and most of the measurements were performed at ~ 2 K. The crystals were mounted with the $\langle 100 \rangle$ axis vertical and the front face perpendicular to the incident light. Dichroic absorption spectra were obtained with a scanning monochromator Spex Minimate 2 using a plastic linear polarizer. When the time dependence of the absorption was measured at a single wavelength, the light source and monochromator were replaced by a He-Ne laser of approximately 10 mW. The polarization, selected by a calcite prism, was rotated either by a Fresnel rhomb or by a Pockel cell when a fast switching time was needed. In the emission measurements, as sketched in the lower part of Fig. 4, we used a collinear excitation and detection geometry, with an InSb ir detector of the $2.7\text{-}\mu\text{m}$ luminescence and proper filtering out of the exciting radiation. In a few experiments, a Kr^+ -ion laser was used for the excitation.

IV. RESULTS AND DISCUSSION

The measurement of the dichroic absorption spectrum of the $F_A(\text{II})$ centers in $\text{KCl}:\text{Li}^+$ is a direct way of studying the reorientation processes, and it has been extensively used in previous measurements.² Figure 5 shows the dichroic spectra measured at 2 K with light polarized along the y and the x axes of the crystal, after a thorough irradiation of the sample with x -polarized F_{A1} light directed along the z axis. The centers are aligned as shown in Fig. 2(a). Analogously, Figure 6 shows the dichroic spectra measured at 2 K with light polarized along the y and x

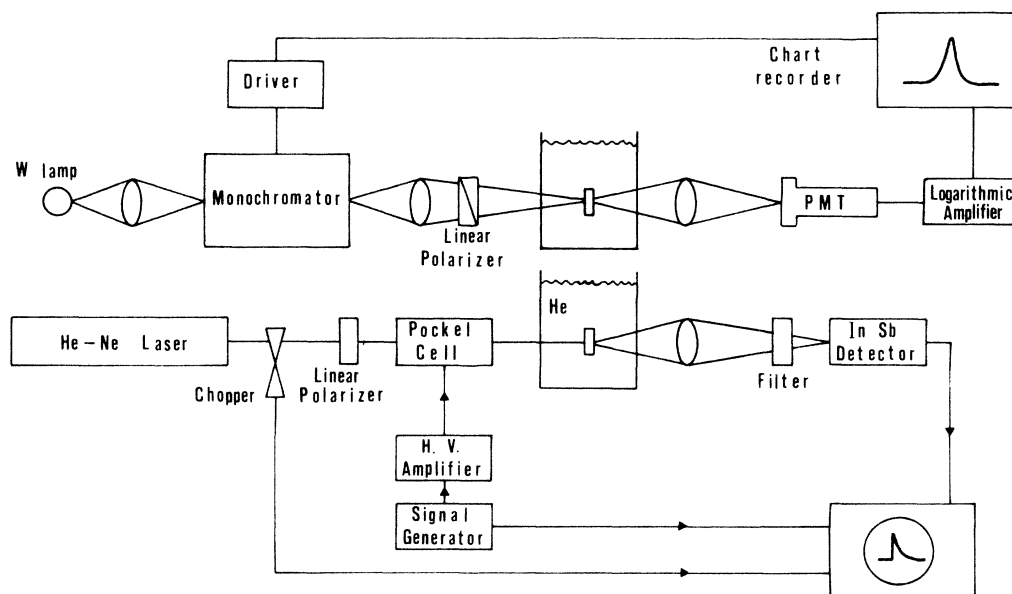


FIG. 4. Experimental setup used to measure the stationary absorption spectra (upper panel) and the kinetic processes (lower panel). (PMT denotes photomultiplier tube and HV high voltage.)

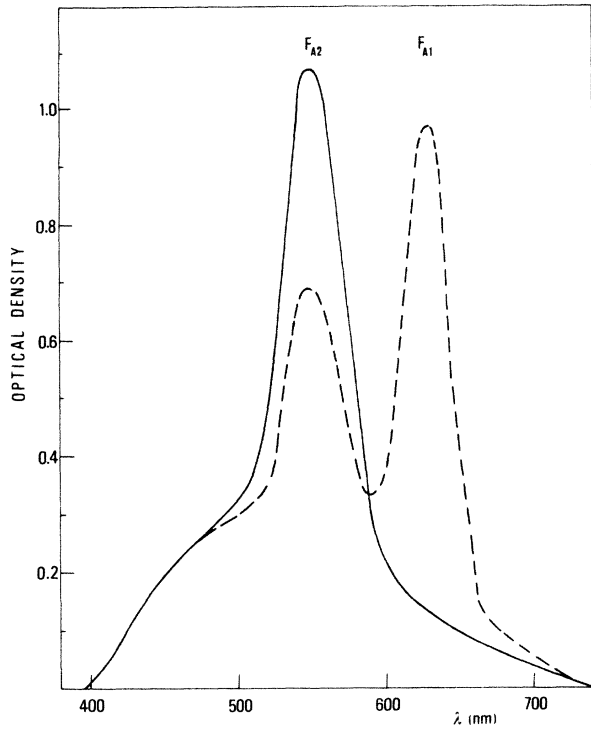


FIG. 5. Dichroic absorption spectra of F_A centers in $\text{KCl}:\text{Li}^+$ at 2 K after irradiation with F_{A1} light linearly polarized along the x axis: —, observed with x -polarized light; - - -, observed with y -polarized light.

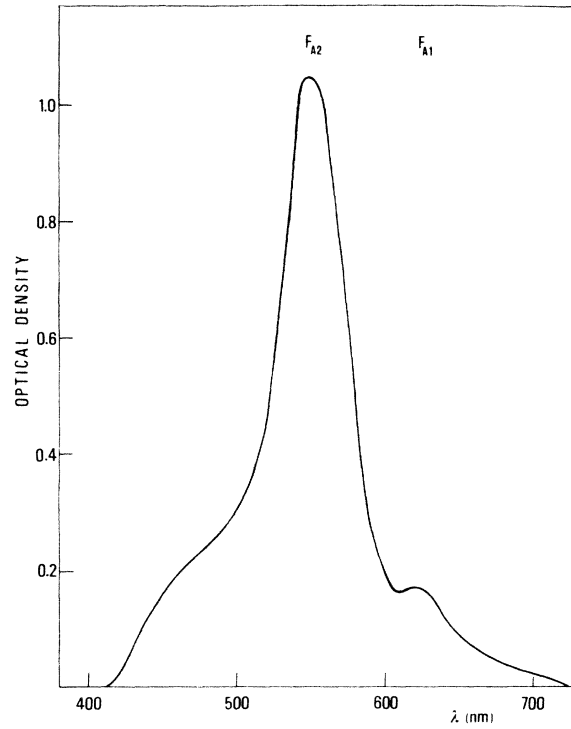


FIG. 6. Dichroic absorption spectra of F_A centers in $\text{KCl}:\text{Li}^+$ at 2 K after irradiation with F_{A1} light polarized at 45° in the x - y plane, observed with x - and y -polarized light: the two curves are completely superimposed.

axes after a thorough irradiation of the sample with light polarized at $\xi = \pi/4$. The centers are aligned as shown in Fig. 2(b). Figures 5 and 6 clearly show how difficult it is to evaluate from absorption measurements the residual absorption of the F_{A1} band after alignment, because of effects due to the absorption background. Therefore, while absorption measurements are indicated whenever a relative measure is necessary, or when a low excitation is requested to avoid perturbation of the system by the probe beam, emission measurements are preferred in all other cases.

We made three different experimental investigations in order both to test the correctness of the rate equations (1) and to obtain reliable values for the off-axis angle θ . The three investigations correspond to the three schemes evaluated in the theoretical section. They will be called steady-state emission, transient emission, and kinetic absorption methods, based on the way they have been carried out.

A. Steady-state emission experiment

In the first case considered in Sec. II the absorption or the emission must be measured in the stationary state while pumping with radiation polarized at a variable angle ξ . In this case the crystal will always be bleached by the exciting light so that the absorption will be small and not easily measurable. As a consequence, luminescence measurements have been preferred. Also, because of the small absorption of the crystal, after the equilibrium is

reached, the intensity of the pumping light is almost constant along the crystal, so that no corrections are needed on expression (7).

Experiments have been made by using a He-Ne laser ($\lambda = 632.8$ nm). The exciting wavelength is in the F_{A1} band and well outside the F_{A2} band, at least at low temperatures, as we will show below. Figure 7 shows the

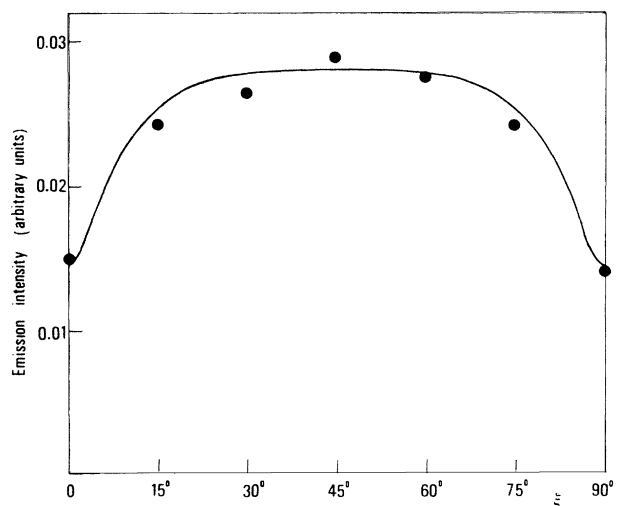


FIG. 7. Angular dependence of the stationary emission intensity under polarized excitation: the solid curve is the theoretical fitting of the experimental points.

luminescence of a sample as a function of the angle ξ . The experimental points are in good agreement with the theoretical curve, Eq. (7), calculated for a value of $\theta=8^\circ$. An analogous experiment has been performed with a krypton laser ($\lambda=649$ nm). In this case the polarization was rotated continuously at a fixed frequency and the luminescence signal was analyzed by a computer, which at the same time performs a best-fitting procedure with formula (7). Preliminary results obtained in this way are in substantial agreement with those just described.

B. Transient effects

Emission measurements have been also performed in the second experimental scheme, where the initial and final values of a reorientation process have to be measured at $\xi=\pi/2$ after a steady preparation of the sample at $\xi=0^\circ$. Figure 8 gives an example of experimental results of luminescence as a function of time for different incident powers. From such measurements it is possible to extract the values of the luminescence at the beginning of the process, $L(0)$, and at the end, $L(\infty)$. The ratio between them, identical to that of the absorption coefficients, is a function of the off-axis angle, given by Eq. (10). However, in this case the intensity of the incident radiation is not constant throughout the sample, and we have to take into account its absorption α . The luminescence emitted by an infinitesimal element of thickness dz

of the crystal is given by

$$dL = cI_0 e^{-\alpha z} \alpha dz, \quad (16)$$

where c is the quantum efficiency of the phenomenon. The total luminescence is easily obtained by integrating the previous expression [Eq. (16)] over the thickness d of the crystal:

$$L = \int_0^d dL = cI_0(1 - e^{-\alpha d}). \quad (17)$$

Thus, if $\alpha_t(0)$ and $\alpha_t(\infty)$ are the absorption coefficients at the beginning and at the end of the reorientation process, we have

$$\frac{L(\infty)}{L(0)} = \frac{1 - e^{-\alpha_t(\infty)d}}{1 - e^{-\alpha_t(0)d}}. \quad (18)$$

Taking into account that, in all the experiments performed, $\alpha_t(\infty)d \ll 1$, one obtains

$$\frac{L(\infty)}{L(0)} \cong \frac{\alpha_t(\infty)}{\alpha_t(0)} \frac{\alpha_t(0)d}{1 - e^{-\alpha_t(0)d}} = \frac{3 \sin^2 \theta}{1 + \cos^2 \theta} \frac{\alpha_t(0)d}{1 - e^{-\alpha_t(0)d}}, \quad (19)$$

where we have used Eq. (10) for the absorption ratio at constant intensity. This result differs from Eq. (10) by a correction factor, easily measurable at the beginning of the experiment. Experimental results using various sources and various pumping intensities give the average value $\theta=9.5^\circ$.

C. Kinetic measurements

Using the two previous methods, we have measured values of the emission intensity and absorption coefficient, completely neglecting the time dependence of the reorientation processes. However, we have shown in Sec. II that the time constants in Eqs. (4) have a strong dependence on θ . If we start from a situation with almost all the centers aligned along the z axis, Fig. 2(b), we can reorient them along the x axis by pumping the system with light polarized along the y axis. The population along the x axis increases in an exponential way, Eq. (11), and can be monitored by absorption measurements with very weak light. In practice, the same light source (lamp or He-Ne laser) was used to pump and to monitor. For this latter purpose, the polarization is rotated by $\pi/2$ and the intensity strongly attenuated. Typical experimental results obtained with a He-Ne laser are reported in Fig. 9 for three different temperatures. Fittings of the experimental points with formula (11) show satisfactory agreement. In this way it is possible to extract the value of the "slow" time constant T_S . In these measurements the intensity of the pumping light is almost constant along the sample, because the centers cannot be reoriented along the y axis. In contrast, a correction is necessary for the measure of the "fast" time constant. Indeed, in this case the centers initially oriented along the y and x axes, Fig. 2(a), are pumped out of the y axis, by the same beam used in the measurement of the slow process. At this time, however, one observes a large variation of the light transmitted through the crystal, due to the change of the absorption

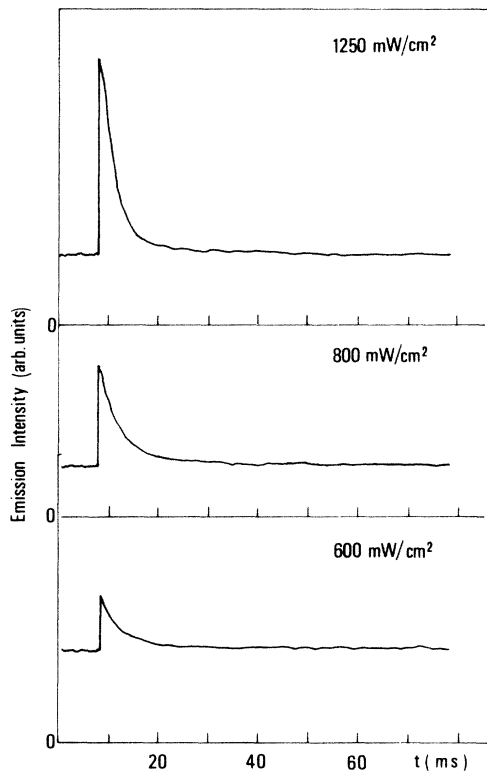


FIG. 8. Reorientation time of F_A centers for various powers of the incident F_{A1} light: see text for details.

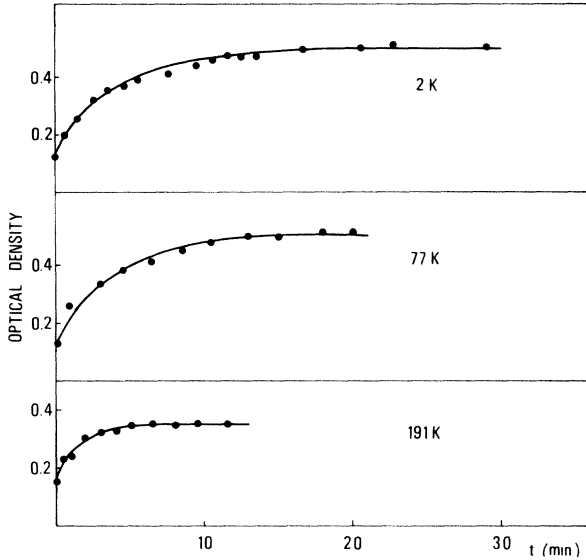


FIG. 9. Realignment of F_A centers along the x axis under y -polarized pumping of the crystal prepared as shown in Fig. 2(b): the solid curves are theoretical fittings of the experimental points.

coefficient during the center's reorientation. The change of the beam intensity through an infinitesimal element of thickness dz of the crystal is given by

$$dI(z,t) = -\alpha(z,t)I(z,t)dz. \quad (20)$$

From Eq. (13) we know that

$$\alpha(z,t) = \frac{N\sigma_0}{2} e^{-\eta I(z,t)\sigma_0 t}, \quad (21)$$

so that

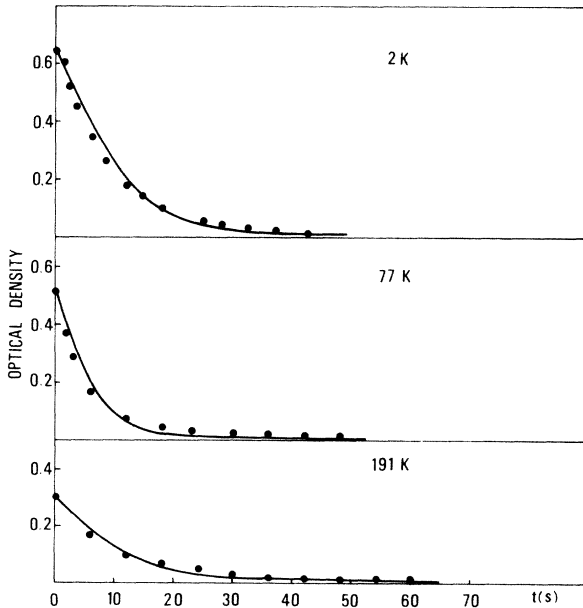


FIG. 10. Decrease of F_A centers aligned along the y axis under y -polarized pumping of the crystal prepared as shown in Fig. 2(a): the solid curves are theoretical fittings of the experimental points.

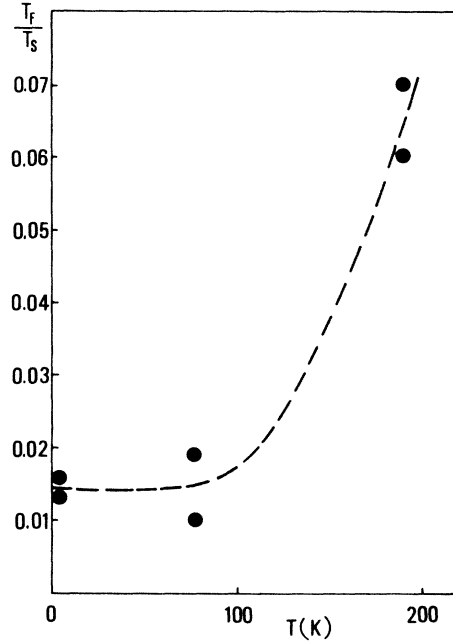


FIG. 11. Temperature dependence of the ratio of the fast and slow reorientation time constants.

$$dI(z,t) = -\frac{N\sigma_0}{2} I(z,t) e^{-\eta I(z,t)\sigma_0 t} dz. \quad (22)$$

Integration of Eq. (22) along the thickness d of the sample, performed by a computer, facilitates comparison of the theoretical values to the experimental data of $I(d,t)$ and, from them, evaluation of the "fast" time constant T_F . In Fig. 10 we report some fast reorientational processes obtained with a He-Ne laser. Fittings made using Eq. (22) are also shown. It is evident that the behavior is not exponential as expected, because I is not constant along the crystal. As we have shown before, from the ratio of the slow and fast time constants, Eq. (15), it is possible to obtain the off-axis angle $\theta = 8^\circ$.

Using this method we investigated the influence of the long-wavelength tail of the F_{A2} band (see Fig. 5) on the present measurements. In writing the rate equations (1) we have supposed that the two bands F_{A1} and F_{A2} are well separated in energy and we completely neglected the possible contribution of the F_{A2} band to the total absorption at the pumping wavelength. However, it is not possible to exclude *a priori* the possible influence of the F_{A2} band when a source pump like the He-Ne laser is used. Thus we measured the ratio T_F/T_S at various temperatures, since the increase of the width of the absorption band with temperature should produce a strong variation of that ratio in the case of overlapping of the two bands. The experimental results, Fig. 11, show that the ratio

TABLE I. Off-axis angle of the $F_A(\text{II})$ center in $\text{KCl}:\text{Li}^+$ measured by different optical methods.

Methods	θ (deg)
Steady-state emission	8.0 ± 1.0
Transient emission	9.5 ± 2.0
Kinetics of absorption	8.0 ± 1.0

T_F/T_S is constant up to 80 K and increases markedly only above that temperature. We conclude that at low temperature the F_{A1} and F_{A2} bands are well separated and that their overlap is negligible at the wavelength of the pumping light. Only above 80 K is the pumping light absorbed by both F_{A1} and F_{A2} bands, completely changing the kinetics of the reorientation process.

Up to now we have assumed that the crystal plane (001) is normal to the incident light so that the reference frame of Fig. 3 can be used. However, we have investigated the magnitude of a possible geometrical error by using the dynamic absorption method. More exactly, we have measured the ratio T_F/T_S as a function of the angle ϕ between the direction of propagation of the pumping beam light and the z axis in the plane y - z . By using the same procedure as that used to obtain the previous cross sections, given by formulas (3), we have, in this case,

$$\begin{aligned} \sigma_x &= \sigma_0 \frac{\sin^2\theta \cos^2\phi + \sin^2\theta \sin^2\phi}{2}, \\ \sigma_y &= \sigma_0 \left[\cos^2\theta \cos^2\phi + \frac{\sin^2\theta \sin^2\phi}{2} \right], \\ \sigma_z &= \sigma_0 \left[\frac{\sin^2\theta \cos^2\phi}{2} + \cos^2\theta \sin^2\phi \right]. \end{aligned} \quad (23)$$

By calculating A and Δ as functions of the new cross sections (23) and by assuming a small angle of incident ϕ , we obtain

$$T_F/T_S \simeq \frac{3}{4}(\sin^2\theta + \sin^2\phi \cos^2\phi), \quad (24)$$

which reduces to Eq. (15) for $\phi=0^\circ$.

In Fig. 12 we have reported the experimental ratio T_F/T_S for several values of the angle ϕ . A fitting of Eq. (24) shows that there is a mismatch of 1.5° between the measured angle of incidence and the direction normal to the crystal. This experiment shows that the ratio T_F/T_S is not strongly dependent on the angle ϕ . It gives a minimum value of T_F/T_S similar to those obtained previously, and the best agreement is obtained for $\theta=8^\circ$.

The values of the off-axis angle θ of the $F_A(\text{II})$ center in KCl:Li⁺ measured with the different methods are reported in Table I. These values are in substantial agreement with those published in our preliminary reports^{17,18} and only somewhat larger than the value $\theta=2.5^\circ$ quoted by Lüty.¹⁹ The spread among the different measurements can be probably reduced by a tighter control of the geometry of the setup.

V. CONCLUSIONS

The optical experiments we have reported completely confirm the symmetry properties of the $F_A(\text{II})$ center in KCl:Li⁺ and indicate that the most probable value of the off-axis angle is $\theta=8^\circ$, obtained through measurements of the static and transient emission and of the kinetics of the absorption changes during the reorientation processes. We have shown that photostimulated reorientation can provide useful information on the off-axis properties of the F_A center and, we believe, of other systems as well.

The importance of the alignment of the dipolar centers and of the residual absorption or luminescence can be of great importance in the color-center lasers. We have already shown that by maximizing with proper polarization

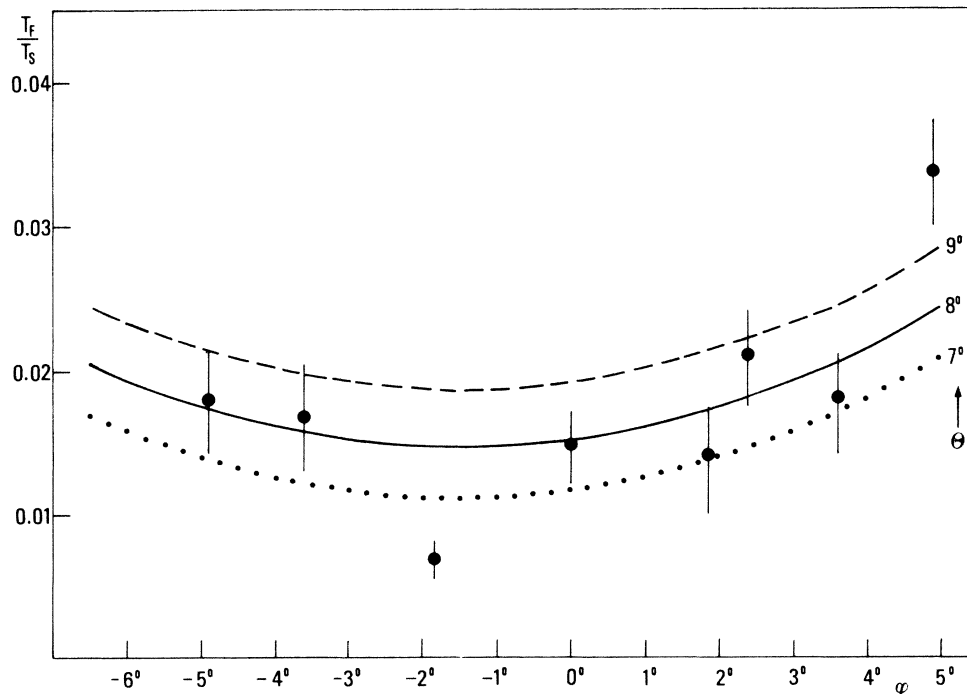


FIG. 12. Dependence of the reorientation time constants on the angle of incidence ϕ of the pumping beam on the crystal. The three curves have been calculated from Eq. (24) for different values of the off-axis angle θ .

the number of absorbing centers without alignment losses, the output of an $F_A(\text{Li})$ laser can increase by nearly an order of magnitude with a parallel reduction of the pump threshold.²⁰ A thorough understanding of the physics of the centers used in the color-center laser will undoubtedly lead to a marked improvement of the performance of this class of lasers.

ACKNOWLEDGMENTS

The contributions of Dr. A. Tiourine (University of Odessa, U.S.S.R.) and of Professor P. Minguzzi (Universi-

ty of Pisa, Italy) are gratefully acknowledged. The authors thank P. Cardoni, I. Cenciarelli, L. Mori, and G. Schina (Laboratory of Molecular Spectroscopy, ENEA), and A. Miriametro, R. Moretto, and F. Stazi (Physics Department, University "La Sapienza"), for their valuable technical assistance, and A. Pieralisi for her collaboration. This work was partially supported by the Consiglio Nazionale delle Ricerche and by the Ministero della Pubblica Istruzione through the Gruppo Nazionale di Struttura della Materia.

*Present address: Dipartimento di Struttura della Materia dell' Università, Napoli, Italy.

†Present address: Istituto di Fisica dell' Università, Siena, Italy.

¹W. B. Fowler, in *Physics of Color Centers*, edited by W. B. Fowler (Academic, New York, 1968), Chap. 2.

²F. Lüty, in *Physics of Color Centers*, Ref. 1, Chap. 3.

³For a detailed survey on the color-center laser systems and devices, see L. F. Mollenauer, *Methods of Experimental Physics*, edited by C. L. Tang (Academic, London, 1979), Vol. 15, Pt. B, p. 1.

⁴W. Gellerman, C. R. Pollock, and F. Lüty, *Opt. Commun.* **39**, 391 (1981).

⁵I. Schneider, *Opt. Lett.* **7**, 271 (1981).

⁶B. Fritz and E. Menke, *Solid State Commun.* **3**, 61 (1965).

⁷L. F. Mollenauer and D. H. Olson, *Appl. Phys. Lett.* **24**, 386 (1974).

⁸A. H. Harker and J. M. Vail, *Phys. Status Solidi B* **108**, 87 (1981).

⁹A. M. Stoneham, *Theory of Defects in Solids* (Clarendon, Ox-

ford, 1975), Chap. 21.

¹⁰J. A. D. Matthew, *Solid State Commun.* **3**, 365 (1965).

¹¹V. Narayanamurti and R. O. Pohl, *Rev. Mod. Phys.* **42**, 201 (1970).

¹²B. Fritz, in *Localized Excitation in Solids*, edited by R. F. Wallis (Plenum, New York, 1968), p. 496.

¹³F. Rosenberger and F. Lüty, *Phys. Rev. Lett.* **21**, 25 (1968).

¹⁴F. Rosenberger and F. Lüty, *Solid State Commun.* **7**, 983 (1969).

¹⁵Y. Mori and H. Ohkura, *J. Phys. Soc. Jpn.* **50**, 1421 (1981).

¹⁶H. Holland and F. Lüty, *Phys. Status Solidi B* **89**, K73 (1978).

¹⁷G. Baldacchini, G. P. Gallerano, U. M. Grassano, M. Meucci, A. Scacco, F. Somma, A. Tiourine, and M. Tonelli, *Phys. Status Solidi B* **122**, K83 (1984).

¹⁸G. Baldacchini, U. M. Grassano, M. Meucci, A. Scacco, F. Somma, and M. Tonelli, *J. Lumin.* **31-32**, 154 (1984).

¹⁹F. Lüty, *Surf. Sci.* **37**, 120 (1973).

²⁰M. Meucci, M. Tonelli, G. Baldacchini, U. M. Grassano, A. Scacco, and F. Somma, *Opt. Commun.* **51**, 33 (1984).